

## Article

# The Dynamic Changes of Alternative Electron Flows upon Transition from Low to High Light in the Fern *Cyrtomium fortune* and the Gymnosperm *Nageia nagi*

Jun-Bin Cheng <sup>1,2</sup> , Shi-Bao Zhang <sup>1</sup>, Jin-Song Wu <sup>1</sup> and Wei Huang <sup>1,\*</sup> <sup>1</sup> Kunming Institute of Botany, Chinese Academy of Sciences, Kunming 650201, China<sup>2</sup> University of Chinese Academy of Sciences, Beijing 100049, China

\* Correspondence: huangwei@mail.kib.ac.cn

**Abstract:** In photosynthetic organisms except angiosperms, an alternative electron sink that is mediated by flavodiiron proteins (FLVs) plays the major role in preventing PSI photoinhibition while cyclic electron flow (CEF) is also essential for normal growth under fluctuating light. However, the dynamic changes of FLVs and CEF has not yet been well clarified. In this study, we measured the P700 signal, chlorophyll fluorescence, and electrochromic shift spectra in the fern *Cyrtomium fortune* and the gymnosperm *Nageia nagi*. We found that both species could not build up a sufficient proton gradient ( $\Delta pH$ ) within the first 30 s after light abruptly increased. During this period, FLVs-dependent alternative electron flow was functional to avoid PSI over-reduction. This functional time of FLVs was much longer than previously thought. By comparison, CEF was highly activated within the first 10 s after transition from low to high light, which favored energy balancing rather than the regulation of a PSI redox state. When FLVs were inactivated during steady-state photosynthesis, CEF was re-activated to favor photoprotection and to sustain photosynthesis. These results provide new insight into how FLVs and CEF interact to regulate photosynthesis in non-angiosperms.

**Keywords:** energy balancing; ferns; gymnosperms; photoprotection; photosynthesis

**Citation:** Cheng, J.-B.; Zhang, S.-B.; Wu, J.-S.; Huang, W. The Dynamic Changes of Alternative Electron Flows upon Transition from Low to High Light in the Fern *Cyrtomium fortune* and the Gymnosperm *Nageia nagi*. *Cells* **2022**, *11*, 2768. <https://doi.org/10.3390/cells11172768>

Academic Editor: Marek Zivcak

Received: 12 July 2022

Accepted: 22 August 2022

Published: 5 September 2022

**Publisher's Note:** MDPI stays neutral with regard to jurisdictional claims in published maps and institutional affiliations.



**Copyright:** © 2022 by the authors. Licensee MDPI, Basel, Switzerland. This article is an open access article distributed under the terms and conditions of the Creative Commons Attribution (CC BY) license (<https://creativecommons.org/licenses/by/4.0/>).

## 1. Introduction

Under natural conditions, light intensity that is exposed to leaves changes dynamically owing to wind, cloud, and shading from upper leaves or neighboring plants; such light condition is called fluctuating light (FL) [1]. During FL, electron flow from photosystem II (PSII) immediately increases upon an abrupt increase in illumination [2]. Concomitantly, CO<sub>2</sub> fixation needs more time to become fully activated [3], leading to the accumulation of electrons in photosystem I (PSI) electron carriers [4]. If the excess electrons in PSI could not be consumed immediately, reactive oxygen species would generate owing to the electron transfer from reduced P700 to O<sub>2</sub>, causing oxidative damage to the PSI [5–7]. The extent of PSI photoinhibition that is induced by FL could be affected by the background low light [7], the intensity of high light [6], and the frequency of low/light cycle [8,9]. Owing to the key role of PSI in the regulation of photosynthesis, PSI photoinhibition strongly suppresses CO<sub>2</sub> fixation and plant growth [10–14]. Therefore, photoprotection for PSI is fundamental to plant growth under FL [15,16].

PSI over-reduction occurs only when the rate of electron flow from PSII to PSI exceeds the rate of electron sink downstream of PSI [16,17]. Therefore, the PSI redox state can be optimized by donor side regulation and acceptor side regulation [6]. In donor side regulation, the down-regulation of electron flow at either PSII or the cytochrome b6f complex can decrease excitation pressure to PSI and thus alleviate PSI over-reduction [17,18]. In acceptor side regulation, the enhancement of the electron sink downstream of PSI can consume the excess electrons in PSI and thus converts reduced P700 into oxidized P700 [6,19,20]. Flavodiiron proteins (FLVs) consume the excess reducing power in PSI

through photo-reduction of  $O_2$ , showing that FLVs protect PSI through acceptor side regulation [16,21]. Meanwhile, the alternative electron flow that is mediated by FLVs is coupled with the formation of  $\Delta pH$  [16]. As a high  $\Delta pH$  restricts the plastoquinol oxidation and thus slows down the electron transport at the cytochrome b6f complex [22,23], FLVs might protect PSI through donor side regulation. Some studies have proposed that the functional time of FLVs was shorter than 10 s in the model moss *Physcomitrella patens* [16,24]. However, we recently found that the gymnosperm species *Ginkgo biloba* did not generate a sufficient  $\Delta pH$  within the initial 10 s after any increase in illumination [25]. Under such conditions, the operation of FLVs-dependent photoreduction of  $O_2$  was crucial for P700 oxidation and PSI photoprotection. These controversial results require further study to clarify the dynamic change of FLVs activity under FL.

The roles of FLVs in PSI photoprotection have been widely studied in cyanobacteria [26], green algae [27], mosses [16,21,28], and liverworts [29]. However, little is known about the action kinetics of FLVs in ferns and gymnosperms. In *P. patens*, leaves were composed of monolayer cells without stomata. By comparison, stomatal conductance is an important limitation that is imposed to photosynthesis in ferns and gymnosperms [30,31]. We recently found that decreased stomatal conductance led to stronger and prolonged PSI over-reduction under FL in tomato (*Solanum lycopersicum*) and common mulberry (*Morus alba*) [32]. To prevent the risk of PSI over-reduction under FL, the FLVs-dependent electron sink might work longer in ferns and gymnosperms than in *P. patens*.

In angiosperms FLVs are lost during evolution but cyclic electron flow (CEF) around PSI is conserved to sustain photosynthesis under FL [6,15] and other environmental stresses [33–37]. There are two major pathways that are responsible for the operation of CEF, PGR5/PGRL1 and NDH [38–42]. If PGR5/PGRL1-dependent CEF was impaired in angiosperms such as *Arabidopsis thaliana* and rice (*Oryza sativa*), the  $\Delta pH$  formation would be suppressed under high light, causing PSI over-reduction and thus resulting in severe PSI photoinhibition [6,15,43]. Recent studies indicated that CEF was highly activated upon a transition from low to high light in angiosperms [7,44]. The CEF-dependent  $\Delta pH$  formation not only slows down the electron flow at the cytochrome b6f complex but also enhances electron downstream of PSI through increasing the ATP/NADPH production ratio [6]. Therefore, CEF strengthens donor side regulation and accelerates acceptor side regulation, both of which alleviate PSI over-reduction under FL. Opposite to angiosperms, the single loss of the PGR5/PGRL1 pathway hardly affected photosynthesis and plant growth under FL in *P. patens* [21], while double losses of PGR5/PGRL1 and NDH pathways strongly accelerated PSI photoinhibition and impaired plant growth [28]. These results indicated that CEF is also indispensable for sustaining photosynthesis and growth under FL in non-angiosperms. However, the dynamic change of CEF under FL and its relationship to  $\Delta pH$  formation in non-angiosperms have not yet been clarified. In particular, it is unclear how CEF and FLVs interact to regulate photosynthesis under FL.

In addition to photoprotection, CEF regulates the energy balancing in response to a changing environment [45]. Based on the assumption that  $CO_2$  diffusion conductance is higher in *P. patens* than in ferns and gymnosperms, a relatively lower chloroplast  $CO_2$  concentration leads to the increase of photorespiration in ferns and gymnosperms. As the energy budget that is required by photorespiration should be balanced by CEF, a relatively lower CEF activity in *P. patens* can satisfy its low capacity of photorespiration. This note was supported by a gradual decrease of CEF activity after an increase in illumination in *P. patens* [24]. By comparison, the high levels of photorespiration in ferns and gymnosperms [31] requires a higher ATP/NADPH production ratio than in *P. patens*. Therefore, we speculate that after the transition from low to high light, the changing patterns of CEF activity in ferns and gymnosperms are different from that in the model moss *P. patens*.

In this study, we measured the dynamic responses of PSI, PSII, and electrochromic shift signals under FL in a fern *Cyrtomium fortune* and a gymnosperm *Nageia nagi*. The aims were: (1) to assess how FLVs interact with  $\Delta pH$  to regulate PSI redox state under FL; and (2) to examine whether the changing patterns of FLVs and CEF under FL in these two

species are different from the model moss *P. patens*. Our results strongly indicate that the time courses of FLVs and CEF in these two species are different from *P. patens* but similar to angiosperms. The specific roles of FLVs and CET under FL are discussed.

## 2. Results

### 2.1. Redox Kinetics of P700 after Transition from Dark to Actinic Light

The redox change kinetics of P700 upon transition to actinic light in dark-adapted leaves is a reliable method to assess the photoreduction of O<sub>2</sub> that is mediated by FLVs [46,47]. To confirm the existence of FLVs in *Cyrtomium fortunei* and *Nageia nagi*, we first measured the kinetics of P700 redox after transition from dark to actinic light (1809 photons m<sup>-2</sup> s<sup>-1</sup>) (Figure 1). Both species showed rapid re-oxidation of P700 in 2 s after actinic light was turned on. As the Calvin–Benson cycle was highly inactivated after 60 min dark adaptation, this rapid re-oxidation of P700 was caused by alternative electron downstream of PSI rather than CO<sub>2</sub> fixation and photorespiration. Furthermore, this rapid re-oxidation of P700 was clearly disappeared when it was measured under anaerobic conditions, which was similar to the phenotype in mutants that were impaired with FLVs. Therefore, photoreduction of O<sub>2</sub> that was mediated by FLVs contributed to the rapid oxidation of P700 in *C. fortunei* and *N. nagi* during dark-to-light transition.

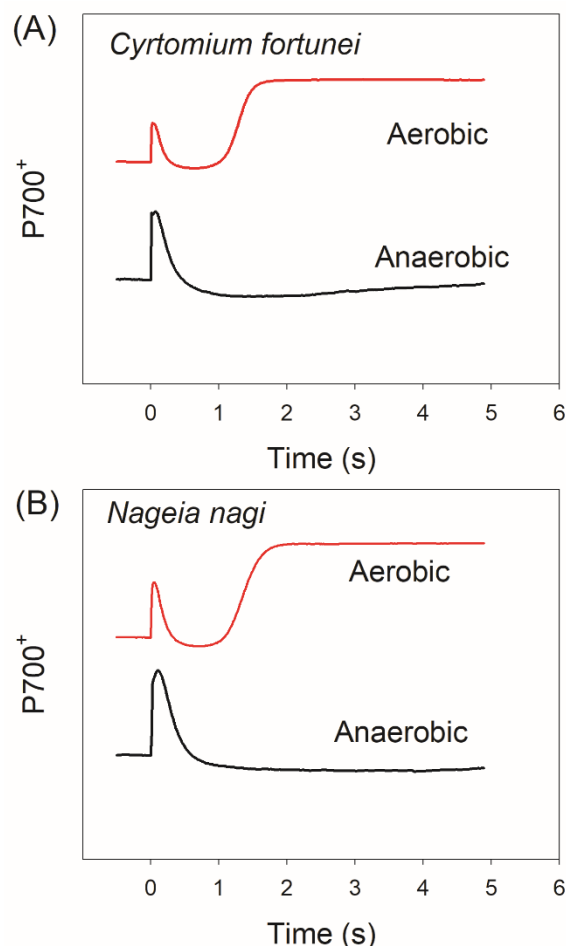


**Figure 1.** Redox kinetics of P700 upon transition from dark to actinic light (1809  $\mu\text{mol photons m}^{-2} \text{s}^{-1}$ ) in leaves of *Cyrtomium fortunei* (A) and *Nageia nagi* (B) measured under aerobic and anaerobic conditions. The data are the means of five independent leaves from five independent plants.

### 2.2. Changes in PSI and PSII Parameters after Transition from Low to High Light

We next measured the kinetics of PSI and PSII parameters under FL. After transition from 59 to 1809  $\mu\text{mol photons m}^{-2} \text{s}^{-1}$ , the quantum yield of PSI photochemistry ( $\Upsilon(\text{I})$ )

sharply decreased in both species (Figure 2A). Concomitantly, the P700 oxidation ratio (Y(ND)) rapidly increased to high levels (>0.8) in 10 s (Figure 2B), leading to low PSI acceptor side limitation (Y(NA)) (<0.1) (Figure 2C). Therefore, the PSI over-reduction was obviously prevented in these two studied species after transition from low to high light. Similar to Y(I), the effective quantum yield of PSII photochemistry (Y(II)) sharply decreased by transitioning to high light (Figure 2D). The non-photochemical quenching (NPQ) was rapidly induced and gradually increased to the maximum over time (Figure 2E), resulting in a low quantum yield of non-regulatory energy dissipation in PSII (Y(NO)) (Figure 2F). After the abrupt increase in illumination, the electron transport rate through PSI (ETRI) rapidly increased and was nearly maintained stable (Figure 3A). Concomitantly, the electron transport rate through PSII (ETR<sub>II</sub>) increased to the peak in approximately 30 s and gradually decreased during the next 90 s (Figure 3B). Therefore, the alternative electron flow that was mediated by FLVs was operational within the initial 20 s after transition from low to high light.

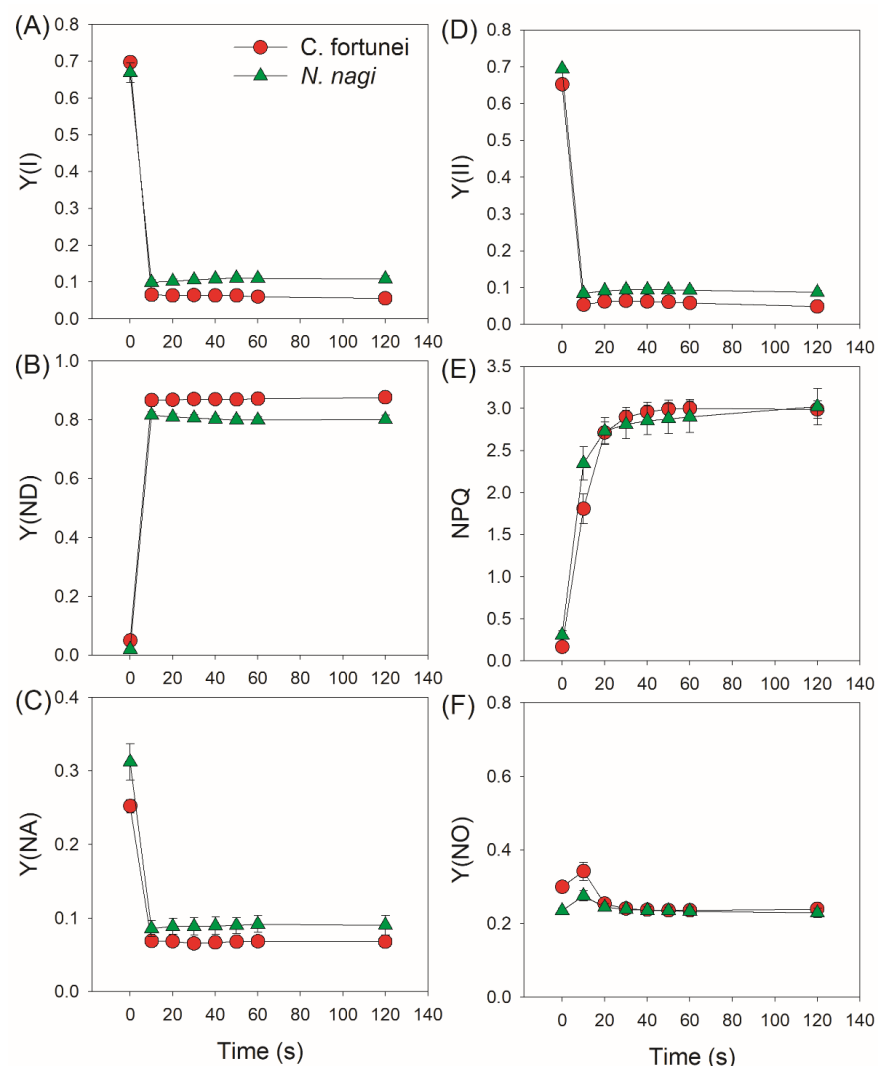


**Figure 2.** Changes in the quantum yields of PSI and PSII after transition from 59 ( $t = 0$ ) to 1809  $\mu\text{mol photons m}^{-2} \text{s}^{-1}$  in leaves of *Cyrtomium fortunei* and *Nageia nagi*. (A) Y(I) represents the quantum yield of PSI photochemistry; (B) Y(ND), the quantum yield of PSI non-photochemical energy dissipation due to donor side limitation; (C) Y(NA), the quantum yield of PSI non-photochemical energy dissipation due to acceptor side limitation; (D) Y(II) represents the quantum yield of PSII photochemistry; (E) NPQ, non-photochemical quenching in PSII; (F) Y(NO), the quantum yield of PSII non-regulatory energy dissipation. The data are the means  $\pm$  SE ( $n = 5$ ).

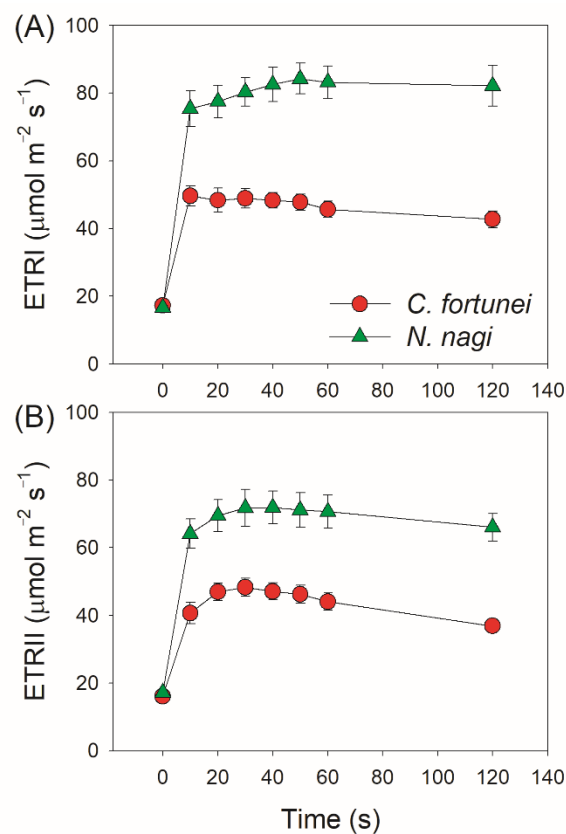


**Figure 3.** Changes in the photosynthetic electron transport rates after transition from 59 ( $t = 0$ ) to 1809  $\mu\text{mol photons m}^{-2} \text{s}^{-1}$  in leaves of *Cyrtomium fortunei* and *Nageia nagi*. (A) ETRI represents electron transport rate through PSI; (B) ETRII, electron transport rate through PSII. The data are the means  $\pm$  SE ( $n = 5$ ).

### 2.3. Changes in $\Delta\text{pH}$ , $g_{\text{H}^+}$ , and CEF after Transition from Low to High Light

As the proton gradient ( $\Delta\text{pH}$ ) across the thylakoid membranes and the activity of thylakoid proton conductance ( $g_{\text{H}^+}$ ) play important roles in photosynthetic regulation under excess light energy, we measured the ECS signals to estimate the kinetics of  $\Delta\text{pH}$  and  $g_{\text{H}^+}$  after transition from low to high light. We found that in *C. fortunei* and *N. nagi*, the values of  $\Delta\text{pH}$  after this light transition for 20 s were significantly lower than those after this light transition for 60 s and 120 s (Figure 4). These results indicated that *C. fortunei* and *N. nagi* could not generate a sufficient  $\Delta\text{pH}$  at least within the initial 20 s after the light intensity increased abruptly. Such insufficient  $\Delta\text{pH}$  might be related to the relatively high  $g_{\text{H}^+}$  (Figure 5). After transition from low to high light,  $g_{\text{H}^+}$  first decreased and finally re-increased (Figure 5). Such a re-increase of  $g_{\text{H}^+}$  suggested that the Calvin–Benson cycle was re-activated. To evaluate the kinetics of CEF under FL, we calculated time courses of the relative proton flux through the thylakoid membrane ( $v_{\text{H}^+}$ ) and the ratio of  $v_{\text{H}^+}/\text{ETRII}$ . After transition from low to high light,  $v_{\text{H}^+}$  and  $v_{\text{H}^+}/\text{ETRII}$  ratio rapidly increased to the peak in 10 s in both species, followed by the rapid decreases in 20 s and the subsequent re-increase in 120 s (Figure 6). These results indicated that CEF was highly stimulated within the first 10 s but rapidly decreased in the subsequent seconds. After the Calvin cycle was highly activated under high light, CEF was re-activated to sustain photosynthesis.

To examine the role of  $\Delta\text{pH}$  in photosynthetic regulation under FL, we plotted the values of  $\Delta\text{pH}$ , NPQ, and  $Y(\text{ND})$  after transition from low to high light. Positive relationships between  $\Delta\text{pH}$  and NPQ were found in both species (Figure 7A), indicating that the gradual increase of  $\Delta\text{pH}$  induced NPQ and thus protected PSII against excess light energy. However, the dynamic changes of  $\Delta\text{pH}$  hardly affected the values of  $Y(\text{ND})$  in both species (Figure 7B), pointing out that in these two non-angiosperms the PSI redox state under

FL was not controlled by  $\Delta\text{pH}$ . Therefore, the dynamic formation of  $\Delta\text{pH}$  under FL had different effects on photoprotection for PSI and PSII in non-angiosperms.

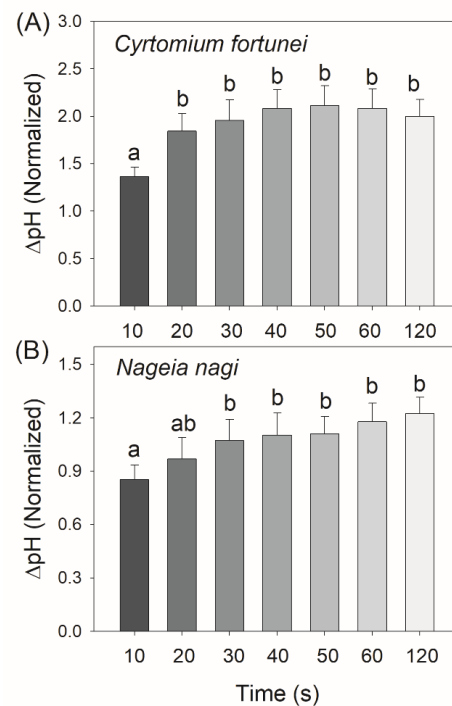


**Figure 4.** Changes in the trans-thylakoid proton gradient ( $\Delta\text{pH}$ ) after transition from 59 to 1809  $\mu\text{mol photons m}^{-2} \text{s}^{-1}$  in leaves of *Cyrtomium fortunei* (A) and *Nageia nagi* (B). All the  $\Delta\text{pH}$  levels were normalized against the magnitude of  $\text{ECS}_{\text{ST}}$ . The data are the means  $\pm$  SE ( $n = 5$ ). Different letters indicate significant differences between the different treatments.

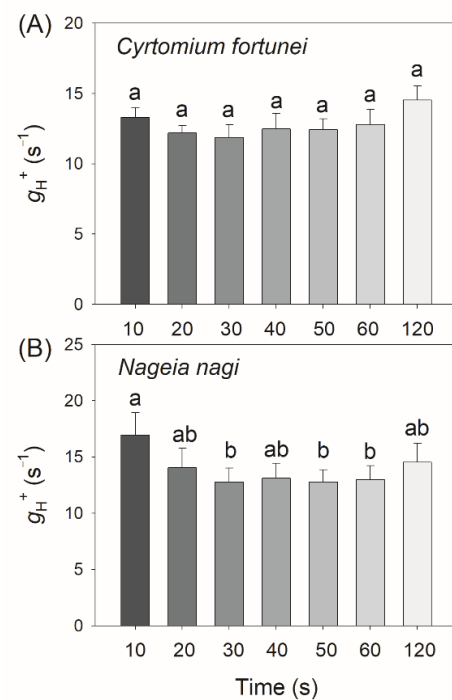


**Figure 5.** Changes in the activity of chloroplast ATP synthase ( $g_{\text{H}^+}$ ) after transition from 59 to 1809  $\mu\text{mol photons m}^{-2} \text{s}^{-1}$  in leaves of *Cyrtomium fortunei* (A) and *Nageia nagi* (B). The data are the means  $\pm$  SE ( $n = 5$ ). Different letters indicate significant differences between the different treatments.

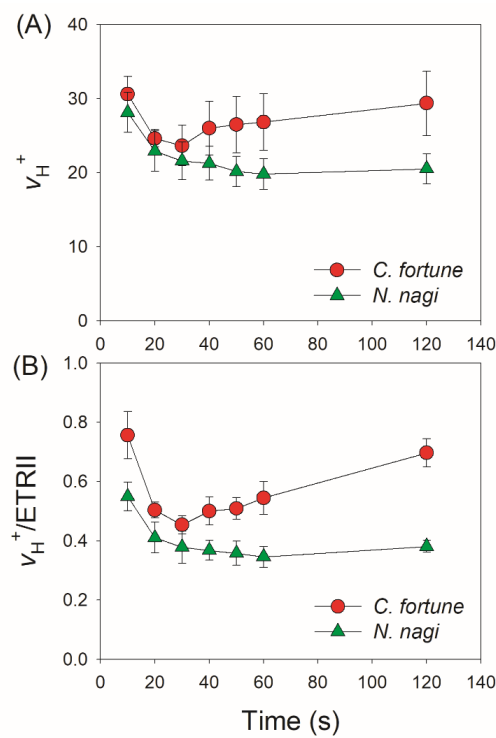


**Figure 6.** Changes in the relative proton flux through the thylakoid membrane ( $v_H^+$ ) (A) and relative CEF (B) after transition from transition from 59 to 1809  $\mu\text{mol photons m}^{-2} \text{s}^{-1}$  in leaves of *Cyrtomium fortune* and *Nageia nagi*. The relative CEF was estimated by the  $v_H^+/\text{ETR}_{II}$  ratio. The data are the means  $\pm$  SE (n = 5).

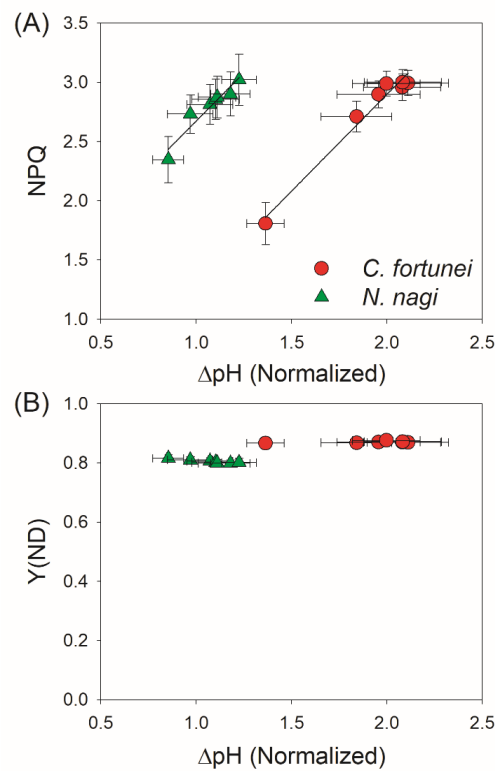


**Figure 7.** Changes in NPQ (A) and Y(ND) (B) as a function of  $\Delta\text{pH}$  after transition from 59 to 1809  $\mu\text{mol photons m}^{-2} \text{s}^{-1}$  in leaves of *Cyrtomium fortune* and *Nageia nagi*. The data are the means  $\pm$  SE (n = 5).

### 3. Discussion

The FLVs-mediated alternative electron sink is operational in photosynthetic organisms except in angiosperms [24,48]. Recent studies have documented the critical roles of FLVs in cyanobacteria, green algae, mosses, and liverworts under FL [16,26,27,29]. In these groups, *flv* mutants showed severe PSI photoinhibition and stunted plant growth if they are exposed to FL [21,28]. However, little is known about the role of FLVs in photosynthetic regulation under FL in the residual other two groups of non-angiosperms, ferns and gymnosperms. Here, we document that FLVs-mediated photoreduction of O<sub>2</sub> contributes to a rapid oxidation of P700 after any increase in light intensity in *Cyrtomium fortune* (fern) and *Nageia nagi* (gymnosperm) (Figures 1 and 2). Furthermore, we found that the action kinetics of FLVs activity were largely correlated with the ΔpH formation. In addition, the role CEF in photosynthetic regulation under FL in them was energy balancing rather than photoprotection.

Although FLV activity is proven to be the one of most important regulators in non-angiosperms when exposed to FL, the specific protection mechanisms have not yet been well clarified. Generally, alternative electron transport that is mediated by FLVs not only enhances electron downstream of PSI but also contributes to the ΔpH formation across the thylakoid membranes. Therefore, some scholars propose that the ΔpH-dependent photosynthetic control at the cytochrome b6f complex is an important mechanism behind how FLVs oxidize P700 under FL [16]. However, this scheme is now challenged by a recent study on the gymnosperm *Ginkgo biloba* [25]. After transition from dark or low light to high light, *G. biloba* did not build up a sufficient ΔpH in 10 s but P700 was highly oxidized, leading to a hypothesis that the ΔpH-dependent photosynthetic control played a minor role in FLVs-mediated P700 oxidation [25]. In the model moss *P. patens*, FLVs-dependent alternative flow was functional in the first seconds up to 10 s but was undetectable during prolonged illumination [16,24]. If the FLV activity just functioned within the first 10 s after light abruptly increased, ETRII would get the first peak within the first 10 s. When FLV activity is inactivated, ETRII will gradually increase owing to the activation of the Calvin cycle [24]. However, we observed that ETRII peaked after transition from low to high light for 30 s in *C. fortune* and *N. nagi*, followed by the subsequent decrease in 120 s (Figure 3B). This result indicated that the action time of FLVs in them lasted at least 30 s. Therefore, the function time of FLVs is likely different among different groups of non-angiosperms.

A question arises why FLVs work longer in *C. fortune* and *N. nagi* than in *P. patens*. One possible explanation is that the work time of FLVs is influenced by the kinetics of ΔpH formation. Many previous studies on angiosperms have documented that ΔpH is the key signal determining the redox state of PSI under high light and FL [38]. For example, if the ΔpH formation was suppressed by the impairment of CEF or enhanced the activity of chloroplast ATP synthase, PSI over-reduction and severe PSI photoinhibition would be observed under FL [49,50]. However, these lethal phenotypes can be rescued by the introduction of FLVs [6]. Furthermore, introduction of FLVs into WT plants of *Arabidopsis thaliana* and rice can prevent PSI over-reduction under FL but do not affect the steady-state photosynthesis [4,51]. Therefore, FLVs activity is particularly seminal when the ΔpH is low but is dispensable under conditions of high ΔpH. In the present study, we found that *C. fortune* and *N. nagi* needed approximately 30 s to accomplish the buildup of ΔpH (Figure 4), which was consistent with the duration time of FLVs activity (Figure 3B). After transition to high light for 120 s, ΔpH was formed sufficiently in *C. fortune* and *N. nagi* (Figure 4). Concomitantly, FLVs was inactivated as indicated by the relatively low ETRII values (Figure 3B). Therefore, after transition from low to high light, FLVs and ΔpH alternately optimize the PSI redox state in non-angiosperms.

Compared with FLVs, CEF plays a weaker role in photoprotection for PSI under FL in the model moss *P. patens* [21]. In *P. patens*, single impairment of the PGR5/PGRL1 pathway hardly affected the PSI activity and plant growth under FL [21], while double impairment of the PGR5/PGRL1 and NDH pathways largely reduced biomass production [28]. Here, we found that in *C. fortune* and *N. nagi*, CEF was stimulated in the first 10 s after an

abrupt increase in illumination (Figure 6B), which was accompanied by an insufficient  $\Delta pH$  (Figure 4). Therefore, CEF probably helped the rapid formation of  $\Delta pH$  under FL in them, which was similar to the phenotypes in angiosperms. Such CEF-dependent  $\Delta pH$  formation favored the induction of NPQ and thus contributed to photoprotection for PSII (Figure 7A). However, unlike the importance of CEF in regulating the PSI redox state under FL in angiosperms, the PSI redox state was not influenced by  $\Delta pH$  because of the weak correlation between P700 oxidation and  $\Delta pH$  (Figure 7B). Therefore, in the presence of FLVs, the rapid oxidation of PSI in *C. fortune* and *N. nagi* was independent of the transient stimulation of CEF.

After transition to high light for 120 s, the relatively stable ETRII was accompanied with the re-increase of CEF activity (Figure 6B). This re-increase of CEF activity contributed to the maintenance of  $\Delta pH$  under constant high light, which balanced the energy budget for primary metabolism. The CEF activity can be regulated by adenylate status. Generally, CEF is activated when the stroma ATP level is low, but it is downregulated when the ATP level increases [52]. Within the first 10 s after transition from low to high light, the low stroma ATP level initiated the transient stimulation of CEF. Subsequently, the operation of FLVs activity increased the stroma ATP level and thus slowed down the CEF activity. Under steady state photosynthesis, the full activation of  $CO_2$  assimilation and the inactivation of FLVs activity decreased the stroma ATP level, which induced the re-activation of CEF to maintain normal adenylate status. Therefore, the dynamic change of CEF activity under FL further explains why CEF is essential for sustaining photosynthesis in non-angiosperms.

In summary, we examined the kinetics of FLVs activity and CEF after transition from low to high light in the fern *C. fortune* and the gymnosperm *N. nagi*. We found that within the first 30 s after light abruptly increased, FLVs were functional to avoid PSI over-reduction under conditions of insufficient  $\Delta pH$ . The functional time of FLVs in *C. fortune* and *N. nagi* was much longer than those in the model moss *P. patens*. CEF was strongly activated within the first 10 s after the light abruptly increased, which played a major role in energy balancing rather than the regulation of the PSI redox state. When FLVs were inactivated during steady-state photosynthesis, CEF was re-activated to favor photoprotection and sustain photosynthesis. These results provide new insights into how FLVs and CEF interact to regulate photosynthesis in non-angiosperms.

## 4. Materials and Methods

### 4.1. Plant Materials

A fern species *Cyrtomium fortunei* J. Sm. (Dryopteridaceae) and a gymnosperm species *Nageia nagi* (Thunberg) Kuntze (Podocarpaceae) were chosen in this study. The plants were grown in a greenhouse at the Kunming Botanical Garden, Yunnan, China (102°44'31" E, 25°08'24" N, 1950 m of elevation). The light conditions were 40% full sunlight (the maximum value was 800  $\mu\text{mol photons m}^{-2} \text{s}^{-1}$ ), day/night air temperatures 30/20 °C, and a relative humidity of approximately 60–70%. The plants were grown in plastic pots. To prevent any water and nutrient stress, the plants were fertilized and watered regularly. Photosynthetic measurements were conducted on mature but not senescent leaves.

### 4.2. P700 Redox Kinetics Measurements

The redox kinetics of P700 was measured using a Dual-PAM 100 measuring system (Heinz Walz, Effeltrich, Germany) by illumination on dark-adapted leaves. After the inactivation of the Calvin–Benson cycle by dark adaptation for at least 60 min, intact leaves were illuminated at 1809  $\mu\text{mol photons m}^{-2} \text{s}^{-1}$  for 5 s under atmospheric air conditions at approximately 25 °C [46].

### 4.3. P700 and Chlorophyll Fluorescence Measurements

P700 and chlorophyll fluorescence were measured simultaneously at 25 °C using a Dual-PAM 100 measuring system (Heinz Walz, Effeltrich, Germany). A saturating pulse (20,000  $\mu\text{mol photons m}^{-2} \text{s}^{-1}$ , 300 ms) was used to measure the maximum fluorescence

intensity ( $F_m$ ) and the maximum photo-oxidizable P700 ( $P_m$ ) after dark adaptation for at least 15 min. Subsequently, 15 min illumination at  $759 \mu\text{mol photons m}^{-2} \text{s}^{-1}$  was conducted to activate photosynthetic electron sinks, and then light intensity was changed to  $59 \mu\text{mol photons m}^{-2} \text{s}^{-1}$  for 5 min. Afterwards, light intensity abruptly increased to  $1809 \mu\text{mol photons m}^{-2} \text{s}^{-1}$ . During the follow-up 2 min, P700 and chlorophyll fluorescence parameters were recorded.

The chlorophyll fluorescence parameters were calculated as follows: the quantum yield of PSII photochemistry,  $Y(\text{II}) = (F_m' - F_s)/F_m'$ ; non-photochemical quenching in PSII,  $\text{NPQ} = (F_m - F_m')/F_m'$ ; the quantum yield of non-regulatory energy dissipation in PSII,  $Y(\text{NO}) = F_s/F_m$ .  $F_m$  and  $F_m'$  were the maximum fluorescence intensity and were recorded after dark and light acclimation, respectively.  $F_s$  is the pre-trigger fluorescence intensity. The PSI parameters were calculated as follows: the quantum yield of PSI photochemistry,  $Y(\text{I}) = (P_m' - P)/P_m$ ; the quantum yield of PSI non-photochemical energy dissipation due to donor side limitation,  $Y(\text{ND}) = P/P_m$ ; the quantum yield of PSI non-photochemical energy dissipation due to acceptor side limitation,  $Y(\text{NA}) = (P_m - P_m')/P_m$ . The photosynthetic electron transport rate was calculated as  $\text{ETRI}$  (or  $\text{ETR}_{\text{II}} = \text{PPFD} \times Y(\text{I})$  [or  $Y(\text{II})] \times 0.84 \times 0.5$ , light absorption is assumed to be 0.84 of the incident irradiance, and 0.5 is the fraction of absorbed light reaching PSI or PSII.

#### 4.4. Electrochromic Shift (ECS) Analysis

The ECS signal was monitored using a Dual PAM-100 that was equipped with a P515/535 emitter-detector module by recording the change in absorbance at 515 nm [53]. Before the ECS measurement, a single turnover flash ( $\text{ECS}_{\text{ST}}$ ) was measured after dark-adaptation for at least 60 min [54]. Subsequently, photosynthetic induction was conducted at  $759 \mu\text{mol photons m}^{-2} \text{s}^{-1}$  for 15 min. Afterward, the leaves were illuminated at  $59 \mu\text{mol photons m}^{-2} \text{s}^{-1}$  for 5 min, and then the ECS signal was recorded after transition to  $1809 \mu\text{mol photons m}^{-2} \text{s}^{-1}$  for 10 s. Subsequently, the leaves were repeatedly acclimated to  $59 \mu\text{mol photons m}^{-2} \text{s}^{-1}$  for 5 min, and then the ECS signal was measured after transition to  $1809 \mu\text{mol photons m}^{-2} \text{s}^{-1}$  for 20 s. Similar ECS signals were measured after transition from 59 to  $1809 \mu\text{mol photons m}^{-2} \text{s}^{-1}$  for 30 s, 40 s, 50 s, 60 s, and 120 s. The ECS dark interval relaxation kinetics ( $\text{DIRK}_{\text{ECS}}$ ) were used to calculate the activity of chloroplast ATP synthase ( $g_{\text{H}^+}$ ) and proton gradient ( $\Delta\text{pH}$ ) across the thylakoid membranes [55,56]. All the  $\Delta\text{pH}$  levels were normalized against the magnitude of  $\text{ECS}_{\text{ST}}$ . The relative proton flux through the thylakoid membrane ( $v_{\text{H}^+}$ ) in the light was calculated from the maximal drop in the ECS signal ( $\text{ECS}_{\text{t}}$ ) during a 300-ms  $\text{DIRK}_{\text{ECS}}$  and the value of  $g_{\text{H}^+}$ :  $v_{\text{H}^+} = \text{ECS}_{\text{t}} \times g_{\text{H}^+}$  [56,57]. The relative CEF activation state was estimated by the  $v_{\text{H}^+}/\text{ETR}_{\text{II}}$  ratio.

#### 4.5. Statistical Analysis

Paired *t*-tests were used to determine whether significant differences in  $g_{\text{H}^+}$  and  $\Delta\text{pH}$  existed between the different treatments ( $\alpha = 0.05$ ). The software SigmaPlot 10.0 was used for graphing and fitting.

**Author Contributions:** Conceptualization, W.H. and J.-B.C.; methodology, W.H.; validation, J.-B.C. and W.H.; formal analysis, W.H.; investigation, J.-B.C.; resources, W.H.; writing—original draft preparation, W.H.; writing—review and editing, J.-S.W. and S.-B.Z.; funding acquisition, W.H. and S.-B.Z. All authors have read and agreed to the published version of the manuscript.

**Funding:** This work was supported by the National Natural Science Foundation of China (Grant 31971412).

**Institutional Review Board Statement:** Not applicable.

**Informed Consent Statement:** Not applicable.

**Data Availability Statement:** The data presented in this study are available on request from the corresponding author.

**Conflicts of Interest:** The authors declare no conflict of interest.

## References

1. Percy, R.W. Sunflecks and photosynthesis in plant canopies. *Annu. Rev. Plant Physiol. Plant Mol. Biol.* **1990**, *41*, 421–453. [[CrossRef](#)]
2. Yang, Y.-J.; Zhang, S.-B.; Wang, J.-H.; Huang, W. Photosynthetic regulation under fluctuating light in field-grown *Cerasus cerasoides*: A comparison of young and mature leaves. *Biochim. Biophys. Acta-Bioenerg.* **2019**, *1860*, 148073. [[CrossRef](#)] [[PubMed](#)]
3. Percy, R.W.; Krall, J.P.; Sassenrath-Cole, G.F. Photosynthesis in Fluctuating Light Environments. In *Photosynthesis and the Environment*; Kluwer Academic Publishers: Dordrecht, The Netherlands, 1996; pp. 321–346.
4. Yamamoto, H.; Takahashi, S.; Badger, M.R.; Shikanai, T. Artificial remodelling of alternative electron flow by flavodiiron proteins in *Arabidopsis*. *Nat. Plants* **2016**, *2*, 16012. [[CrossRef](#)] [[PubMed](#)]
5. Kono, M.; Noguchi, K.; Terashima, I. Roles of the cyclic electron flow around PSI (CEF-PSI) and O<sub>2</sub>-dependent alternative pathways in regulation of the photosynthetic electron flow in short-term fluctuating light in *Arabidopsis thaliana*. *Plant Cell Physiol.* **2014**, *55*, 990–1004. [[CrossRef](#)] [[PubMed](#)]
6. Yamamoto, H.; Shikanai, T. PGR5-dependent cyclic electron flow protects photosystem I under fluctuating light at donor and acceptor sides. *Plant Physiol.* **2019**, *179*, 588–600. [[CrossRef](#)]
7. Tan, S.-L.; Huang, J.-L.; Zhang, F.-P.; Zhang, S.-B.; Huang, W. Photosystem I photoinhibition induced by fluctuating light depends on background low light irradiance. *Environ. Exp. Bot.* **2021**, *181*, 104298. [[CrossRef](#)]
8. Qiao, M.-Y.; Zhang, Y.-J.; Liu, L.-A.; Shi, L.; Ma, Q.-H.; Chow, W.S.; Jiang, C.-D. Do rapid photosynthetic responses protect maize leaves against photoinhibition under fluctuating light? *Photosynth. Res.* **2020**, *149*, 57–68. [[CrossRef](#)]
9. Yin, Z.H.; Johnson, G.N. Photosynthetic acclimation of higher plants to growth in fluctuating light environments. *Photosynth. Res.* **2000**, *63*, 97–107. [[CrossRef](#)]
10. Zivcak, M.; Brestic, M.; Kunderlikova, K.; Sytar, O.; Allakhverdiev, S.I. Repetitive light pulse-induced photoinhibition of photosystem I severely affects CO<sub>2</sub> assimilation and photoprotection in wheat leaves. *Photosynth. Res.* **2015**, *126*, 449–463. [[CrossRef](#)]
11. Brestic, M.; Zivcak, M.; Kunderlikova, K.; Sytar, O.; Shao, H.; Kalaji, H.M.; Allakhverdiev, S.I. Low PSI content limits the photoprotection of PSI and PSII in early growth stages of chlorophyll b-deficient wheat mutant lines. *Photosynth. Res.* **2015**, *125*, 151–166. [[CrossRef](#)]
12. Sejima, T.; Takagi, D.; Fukayama, H.; Makino, A.; Miyake, C. Repetitive short-pulse light mainly inactivates photosystem i in sunflower leaves. *Plant Cell Physiol.* **2014**, *55*, 1184–1193. [[CrossRef](#)] [[PubMed](#)]
13. Shimakawa, G.; Miyake, C. What quantity of photosystem I is optimum for safe photosynthesis? *Plant Physiol.* **2019**, *179*, 1479–1485. [[CrossRef](#)] [[PubMed](#)]
14. Lima-Melo, Y.; Gollan, P.J.; Tikkanen, M.; Silveira, J.A.G.; Aro, E.M. Consequences of photosystem-I damage and repair on photosynthesis and carbon use in *Arabidopsis thaliana*. *Plant J.* **2019**, *97*, 1061–1072. [[CrossRef](#)] [[PubMed](#)]
15. Suorsa, M.; Jarvi, S.; Grieco, M.; Nurmi, M.; Pietrzykowska, M.; Rantala, M.; Kangasjarvi, S.; Paakkarinen, V.; Tikkanen, M.; Jansson, S.; et al. PROTON GRADIENT REGULATION5 is essential for proper acclimation of *Arabidopsis* photosystem I to naturally and artificially fluctuating light conditions. *Plant Cell* **2012**, *24*, 2934–2948. [[CrossRef](#)]
16. Gerotto, C.; Alboresi, A.; Meneghesso, A.; Jokel, M.; Suorsa, M.; Aro, E.-M.; Morosinotto, T. Flavodiiron proteins act as safety valve for electrons in *Physcomitrella patens*. *Proc. Natl. Acad. Sci. USA* **2016**, *113*, 12322–12327. [[CrossRef](#)]
17. Tikkanen, M.; Mekala, N.R.; Aro, E.-M. Photosystem II photoinhibition-repair cycle protects Photosystem I from irreversible damage. *Biochim. Biophys. Acta-Bioenerg.* **2014**, *1837*, 210–215. [[CrossRef](#)]
18. Suorsa, M.; Rossi, F.; Tadini, L.; Labs, M.; Colombo, M.; Jahns, P.; Kater, M.M.; Leister, D.; Finazzi, G.; Aro, E.-M.; et al. PGR5-PGRL1-dependent cyclic electron transport modulates linear electron transport rate in *Arabidopsis thaliana*. *Mol. Plant* **2016**, *9*, 271–288. [[CrossRef](#)]
19. Tazoe, Y.; Ishikawa, N.; Shikanai, T.; Ishiyama, K.; Takagi, D.; Makino, A.; Sato, F.; Endo, T. Overproduction of PGR5 enhances the electron sink downstream of photosystem I in a C4 plant, *Flaveria bidentis*. *Plant J.* **2020**, *103*, 814–823. [[CrossRef](#)]
20. Sun, H.; Yang, Y.-J.; Huang, W. The water-water cycle is more effective in regulating redox state of photosystem I under fluctuating light than cyclic electron transport. *Biochim. Biophys. Acta-Bioenerg.* **2020**, *1861*, 148235. [[CrossRef](#)]
21. Storti, M.; Alboresi, A.; Gerotto, C.; Aro, E.; Finazzi, G.; Morosinotto, T. Role of cyclic and pseudo-cyclic electron transport in response to dynamic light changes in *Physcomitrella patens*. *Plant. Cell Environ.* **2019**, *42*, 1590–1602. [[CrossRef](#)]
22. Shikanai, T. Regulatory network of proton motive force: Contribution of cyclic electron transport around photosystem I. *Photosynth. Res.* **2016**, *129*, 253–260. [[CrossRef](#)] [[PubMed](#)]
23. Tikkanen, M.; Aro, E.M. Integrative regulatory network of plant thylakoid energy transduction. *Trends Plant Sci.* **2014**, *19*, 10–17. [[CrossRef](#)] [[PubMed](#)]
24. Alboresi, A.; Storti, M.; Morosinotto, T. Balancing protection and efficiency in the regulation of photosynthetic electron transport across plant evolution. *N. Phytol.* **2019**, *221*, 105–109. [[CrossRef](#)] [[PubMed](#)]
25. Yang, Y.-J.; Sun, H.; Zhang, S.-B.; Huang, W. Roles of alternative electron flows in response to excess light in *Ginkgo biloba*. *Plant Sci.* **2021**, *312*, 111030. [[CrossRef](#)]

26. Allahverdiyeva, Y.; Mustila, H.; Ermakova, M.; Bersanini, L.; Richaud, P.; Ajlani, G.; Battchikova, N.; Cournac, L.; Aro, E.-M. Flavodiiron proteins Flv1 and Flv3 enable cyanobacterial growth and photosynthesis under fluctuating light. *Proc. Natl. Acad. Sci. USA* **2013**, *110*, 4111–4116. [[CrossRef](#)]
27. Jokel, M.; Johnson, X.; Peltier, G.; Aro, E.M.; Allahverdiyeva, Y. Hunting the main player enabling *Chlamydomonas reinhardtii* growth under fluctuating light. *Plant J.* **2018**, *94*, 822–835. [[CrossRef](#)]
28. Storti, M.; Segalla, A.; Mellon, M.; Alboresi, A.; Morosinotto, T. Regulation of electron transport is essential for photosystem I stability and plant growth. *N. Phytol.* **2020**, *228*, 1316–1326. [[CrossRef](#)]
29. Shimakawa, G.; Ishizaki, K.; Tsukamoto, S.; Tanaka, M.; Sejima, T.; Miyake, C. The liverwort, *Marchantia*, drives alternative electron flow using a flavodiiron protein to protect PSI. *Plant Physiol.* **2017**, *173*, 1636–1647. [[CrossRef](#)]
30. Xiong, D.; Douthe, C.; Flexas, J. Differential coordination of stomatal conductance, mesophyll conductance, and leaf hydraulic conductance in response to changing light across species. *Plant. Cell Environ.* **2018**, *41*, 436–450. [[CrossRef](#)]
31. Carriquí, M.; Cabrera, H.M.; Conesa, M.; Coopman, R.E.; Douthe, C.; Gago, J.; Gallé, A.; Galmés, J.; Ribas-Carbo, M.; Tomás, M.; et al. Diffusional limitations explain the lower photosynthetic capacity of ferns as compared with angiosperms in a common garden study. *Plant Cell Environ.* **2015**, *38*, 448–460. [[CrossRef](#)]
32. Li, T.-Y.; Shi, Q.; Sun, H.; Yue, M.; Zhang, S.-B.; Huang, W. Diurnal Response of Photosystem I to Fluctuating Light Is Affected by Stomatal Conductance. *Cells* **2021**, *10*, 3128. [[CrossRef](#)] [[PubMed](#)]
33. Wu, X.; Shu, S.; Wang, Y.; Yuan, R.; Guo, S. Exogenous putrescine alleviates photoinhibition caused by salt stress through cooperation with cyclic electron flow in cucumber. *Photosynth. Res.* **2019**, *141*, 303–314. [[CrossRef](#)] [[PubMed](#)]
34. Wang, P. Chloroplastic NAD(P)H Dehydrogenase in Tobacco Leaves Functions in Alleviation of Oxidative Damage Caused by Temperature Stress. *Plant Physiol.* **2006**, *141*, 465–474. [[CrossRef](#)] [[PubMed](#)]
35. Zhang, R.; Sharkey, T.D. Photosynthetic electron transport and proton flux under moderate heat stress. *Photosynth. Res.* **2009**, *100*, 29–43. [[CrossRef](#)] [[PubMed](#)]
36. Huang, W.; Yang, S.J.; Zhang, S.B.; Zhang, J.L.; Cao, K.F. Cyclic electron flow plays an important role in photoprotection for the resurrection plant *Paraboea rufescens* under drought stress. *Planta* **2012**, *235*, 819–828. [[CrossRef](#)]
37. Strand, D.D.; Livingston, A.K.; Satoh-Cruz, M.; Froehlich, J.E.; Maurino, V.G.; Kramer, D.M. Activation of cyclic electron flow by hydrogen peroxide in vivo. *Proc. Natl. Acad. Sci. USA* **2015**, *112*, 5539–5544. [[CrossRef](#)]
38. Shikanai, T.; Yamamoto, H. Contribution of cyclic and pseudo-cyclic electron transport to the formation of proton motive force in chloroplasts. *Mol. Plant* **2017**, *10*, 20–29. [[CrossRef](#)]
39. Wu, X.; Wu, J.; Wang, Y.; He, M.; He, M.; Liu, W.; Shu, S.; Sun, J.; Guo, S. The key cyclic electron flow protein PGR5 associates with cytochrome b6f, and its function is partially influenced by the LHClI state transition. *Hortic. Res.* **2021**, *8*, 55. [[CrossRef](#)]
40. Munekage, Y.; Hojo, M.; Meurer, J.; Endo, T.; Tasaka, M.; Shikanai, T. PGR5 is involved in cyclic electron flow around photosystem I and is essential for photoprotection in *Arabidopsis*. *Cell* **2002**, *110*, 361–371. [[CrossRef](#)]
41. Munekage, Y.; Hashimoto, M.; Miyake, C.; Tomizawa, K.; Endo, T.; Tasaka, M.; Shikanai, T. Cyclic electron flow around photosystem I is essential for photosynthesis. *Nature* **2004**, *429*, 579–582. [[CrossRef](#)]
42. Shikanai, T.; Endo, T.; Hashimoto, T.; Yamada, Y.; Asada, K.; Yokota, A. Directed disruption of the tobacco *ndhB* gene impairs cyclic electron flow around photosystem I. *Proc. Natl. Acad. Sci. USA* **1998**, *95*, 9705–9709. [[CrossRef](#)] [[PubMed](#)]
43. Yamori, W.; Makino, A.; Shikanai, T. A physiological role of cyclic electron transport around photosystem I in sustaining photosynthesis under fluctuating light in rice. *Sci. Rep.* **2016**, *6*, 20147. [[CrossRef](#)]
44. Yang, Y.-J.; Ding, X.-X.; Huang, W. Stimulation of cyclic electron flow around photosystem I upon a sudden transition from low to high light in two angiosperms *Arabidopsis thaliana* and *Betula striata*. *Plant Sci.* **2019**, *287*, 110166. [[CrossRef](#)] [[PubMed](#)]
45. Walker, B.J.; Strand, D.D.; Kramer, D.M.; Cousins, A.B. The response of cyclic electron flow around photosystem I to changes in photorespiration and nitrate assimilation. *Plant Physiol.* **2014**, *165*, 453–462. [[CrossRef](#)] [[PubMed](#)]
46. Ilík, P.; Pavlovič, A.; Kouřil, R.; Alboresi, A.; Morosinotto, T.; Allahverdiyeva, Y.; Aro, E.M.; Yamamoto, H.; Shikanai, T. Alternative electron transport mediated by flavodiiron proteins is operational in organisms from cyanobacteria up to gymnosperms. *N. Phytol.* **2017**, *214*, 967–972. [[CrossRef](#)] [[PubMed](#)]
47. Takagi, D.; Ishizaki, K.; Hanawa, H.; Mabuchi, T.; Shimakawa, G.; Yamamoto, H.; Miyake, C. Diversity of strategies for escaping reactive oxygen species production within photosystem I among land plants: P700 oxidation system is prerequisite for alleviating photoinhibition in photosystem I. *Physiol. Plant.* **2017**, *161*, 56–74. [[CrossRef](#)]
48. Allahverdiyeva, Y.; Suorsa, M.; Tikkanen, M.; Aro, E.M. Photoprotection of photosystems in fluctuating light intensities. *J. Exp. Bot.* **2015**, *66*, 2427–2436. [[CrossRef](#)]
49. Kanazawa, A.; Ostendorf, E.; Kohzuma, K.; Hoh, D.; Strand, D.D.; Sato-Cruz, M.; Savage, L.; Cruz, J.A.; Fisher, N.; Froehlich, J.E.; et al. Chloroplast ATP Synthase Modulation of the Thylakoid Proton Motive Force: Implications for Photosystem I and Photosystem II Photoprotection. *Front. Plant Sci.* **2017**, *8*, 719. [[CrossRef](#)]
50. Takagi, D.; Amako, K.; Hashiguchi, M.; Fukaki, H.; Ishizaki, K.; Goh, T.; Fukao, Y.; Sano, R.; Kurata, T.; Demura, T.; et al. Chloroplastic ATP synthase builds up a proton motive force preventing production of reactive oxygen species in photosystem I. *Plant J.* **2017**, *91*, 306–324. [[CrossRef](#)]
51. Wada, S.; Yamamoto, H.; Suzuki, Y.; Yamori, W.; Shikanai, T.; Makino, A. Flavodiiron protein substitutes for cyclic electron flow without competing CO<sub>2</sub> assimilation in rice. *Plant Physiol.* **2018**, *176*, 1509–1518. [[CrossRef](#)]

52. Fisher, N.; Bricker, T.M.; Kramer, D.M. Regulation of photosynthetic cyclic electron flow pathways by adenylate status in higher plant chloroplasts. *Biochim. Biophys. Acta-Bioenerg.* **2019**, *1860*, 148081. [[CrossRef](#)]
53. Klughammer, C.; Siebke, K.; Schreiber, U. Continuous ECS-indicated recording of the proton-motive charge flux in leaves. *Photosynth. Res.* **2013**, *117*, 471–487. [[CrossRef](#)] [[PubMed](#)]
54. Wang, C.; Yamamoto, H.; Shikanai, T. Role of cyclic electron transport around photosystem I in regulating proton motive force. *Biochim. Biophys. Acta-Bioenerg.* **2015**, *1847*, 931–938. [[CrossRef](#)] [[PubMed](#)]
55. Sacksteder, C.A.; Kanazawa, A.; Jacoby, M.E.; Kramer, D.M. The proton to electron stoichiometry of steady-state photosynthesis in living plants: A proton-pumping Q cycle is continuously engaged. *Proc. Natl. Acad. Sci. USA* **2000**, *97*, 14283–14288. [[CrossRef](#)] [[PubMed](#)]
56. Cruz, J.A.; Avenson, T.J.; Kanazawa, A.; Takizawa, K.; Edwards, G.E.; Kramer, D.M. Plasticity in light reactions of photosynthesis for energy production and photoprotection. *J. Exp. Bot.* **2005**, *56*, 395–406. [[CrossRef](#)] [[PubMed](#)]
57. Baker, N.R.; Harbinson, J.; Kramer, D.M. Determining the limitations and regulation of photosynthetic energy transduction in leaves. *Plant Cell Environ.* **2007**, *30*, 1107–1125. [[CrossRef](#)] [[PubMed](#)]